Environ Monit Assess (2021) 193: 644
https://doi.org/10.1007/s10661-021-09365-8

Groundwater fluoride concentrations in the watershed sedimentary basin of Quetta Valley, Pakistan

Taimoor Shah Durrani · Abida Farooqi

Received: 23 November 2020 / Accepted: 30 July 2021 / Published online: 13 September 2021

Abstract Litho-geochemical characteristics of low and high fluoride (F^-) groundwater along with hydrological processes were investigated to delineate its genesis and enrichment mechanism in a watershed sedimentary basin. In this study, groundwater F^- concentration ranged from 0 to 20 mg/L with a mean and standard deviation of 2.8 and ± 3.7 mg/L, respectively. Out of $N = 87$, 63% of samples exceeded the World Health Organization (WHO) limit of 1.5 mg/L. The order of cationic and anionic dominance in groundwater samples with mean was found in decreasing order as $Na^+ > Mg^{2+} > Ca^{2+} > K^+$ and $HCO_3^- > SO_4^{2-} > Cl^- > PO_4^{3-} > NO_3^-$ measured in milligrams per liter. Groundwater chemistry changed from Ca-HCO_3 to Na-HCO_3 type and low to high fluoride as we moved from mountain foot towards the synclinal basin. Low fluoride groundwater reflected weathering, recharge, and reverse ion exchange processes with Ca–HCO_3– and Ca–Mg–Cl–type water while high fluoride groundwater revealed base ion exchange, mixing, and desorption as dominant hydrological processes with Na-HCO_3 and Na-Cl types of water. Gibb's diagram showed rock weathering and mineral dissolution as the major geochemical processes controlling water chemistry with an insignificant role of evaporation in the semi-arid area. Fluoride was undersaturated with mineral fluorite, indicating fluoride in groundwater is released by secondary minerals. However, due to complex geological features, groundwater fluoride enrichment was affected by a broad-scale process across a wide area such as depth, residence time, and most important geomorphological units hosting the aquifer.

Keywords Fluoride · Lithological units · Aquifer depth · Principal component · Quetta valley

Introduction

About 1/3rd of the world population lacks access to safe drinking water, and over 80% of diseases occur due to consumption of poor standard water (World Health Organization, 2011). Fluoride (F^-) being a modern toxic agent is used as a quality indicator for safe drinking water. Fluoride is the ionic form of fluorine-F_2 representing the halogen family; it is considered the most reactive, non-metallic, and

Supplementary Information The online version contains supplementary material available at https://doi.org/10.1007/s10661-021-09365-8.

T. S. Durrani (✉) · A. Farooqi (✉)
Hydro-Geochemistry Laboratory, Department of Environmental Sciences, Faculty of Biological Sciences, Quaid-I-Azam University, Islamabad, Pakistan
e-mail: Taimoor.shah@buitms.edu.pk

A. Farooqi
e-mail: afarooqi@qau.edu.pk

T. S. Durrani
Balochistan University of Information Technology Engineering and Management Sciences, Quetta, Pakistan

non-radioactive element in the periodic table. It is one of the richest trace elements and the 13th most abundant element on the earth's crust, with a natural abundance of 0.06 to 0.09% and an average concentration of 0.3 g/kg (Ozsvath, 2009). Fluoride does not exhibit any color, taste, or smell; when dissolved in water, it is found in free and reduced form as negatively charge monovalent ion. Fluoride is considered a double-edged sword due to its lower and upper limits. Depending on the dosage and duration, its effect may range from acute to chronic (Fawell & Bailey, 2006).

Health impacts of F^- from drinking water are maximum as it comprises 75% of daily intake in comparison with sources such as drugs, food, industrial exposure, etc., and because soluble F^- is easily absorbed by the gastrointestinal tract making its bioavailability to 100% (Rao et al., 2021). World Health Organization (WHO) recommends a minimum of 0.7 mg/L for optimal growth and a maximum of 1.5 mg/L as a threshold for F^- content in potable water due to its essentiality as a nutrient. Historically, its health effects trackback to the early nineteenth century, when low fluoride drinking water in Britain was associated with dental caries, followed by another study in the USA where high fluoride drinking water was found to be concomitant to dental fluorosis (Ainsworth, 1933; Dean & Elvove, 1937). High groundwater F^- level of causing fluorosis is becoming a toxicological problem with a global prevalence of 32%, especially in water-stressed countries. In addition, high F^- is likely to produce crippling skeletal fluorosis, hypersensitivity, immunological effects, damage to DNA structure, low children IQ, and cancer; however, this relation is not well linked (Chen et al., 2012; Hu et al., 2021; Rashid et al., 2019a; Zhang et al., 2014).

Fluoride-contaminated groundwater has drawn worldwide consideration due to its substantial impact on human health (Brindha & Elango, 2011; He et al., 2021; Hossain & Patra, 2020; Ozsvath, 2009; Rashid et al., 2018; Su et al., 2019; Wei et al., 2016; Wen et al., 2013). The input and magnitude of groundwater fluoride depend upon its sources. Natural groundwater F^- sources include geothermal activities, volcanic emissions, marine aerosols, marine origin sediments, and fluoride-bearing mineral dissolution such as fluorite, fluorapatite, illite, cryolite, apatite topaz, muscovite, and mica mainly associated with recent quaternary deposit clay minerals (Edmunds & Smedley, 2013; Rashid et al., 2020; Raza et al., 2016). Anthropogenic sources of groundwater F^- contamination reported in various parts of the world include mining, brickworks, aluminum smelting, iron, steel production, cement production, ceramic firing, and agriculture activities (Mukherjee et al., 2015; Rao et al., 2021; Rashid et al., 2018, 2019b). General factors marked for promoting high-fluoride groundwater are fluoride-bearing minerals, pH, residence time, ion exchange, climate, and most importantly aquifer lithological features. Whereas in basins, the provenance and occurrence of groundwater F^- depend chiefly on factors, such as, grain size, topography, primary and secondary porosities of aquifer, slope, recharge patterns, hydraulic conductivity, landform, land use, land cover, climate conditions, depth, and extent of weathering (Chae et al., 2007; Currell et al., 2011; Farooqi et al., 2009; Hu et al., 2016; Kim & Jeong, 2005; Liu et al., 2015; Luo et al., 2018; Saxena & Ahmed, 2001; Selvam, 2015; Su et al., 2019; Wen et al., 2013).

According to Jadhav et al. (2015), in Pakistan, the estimated population exposed to F^--contaminated water is about 2.75 million. When compared with other F^--affected countries such as China, India, Mexico, Egypt, Ethiopia, Saudi Arabia, Nigeria, USA, and Senegal, Pakistan comes 4th after China, India, and Mexico. In Pakistan, a large variation in groundwater F^- has been observed in drinking water as a result of man-made or natural pollution (Farooqi et al., 2009; Naseem et al., 2010; Azizullah et al., 2011; Tahir & Rasheed, 2013; Chandio et al., 2015; Rafique et al., 2015; Rashid et al., 2020). Very high groundwater fluoride concentration (24.4 mg/L) was reported in the study area Quetta Valley by Tahir and Rasheed (2013), but the spatial distribution of such high-fluoride groundwater was unknown. Therefore, to probe lithological influences in basins, the study aims (1) to determine the spatial distribution of groundwater fluoride, (2) to examine depth-dependent variability of groundwater fluoride, and (3) to access the processes and factors controlling fluoride concentration in the aquifer by using well logs data of the area.

Study area

Geographical position and geology

The study area Quetta valley is the capital city of Baluchistan, Pakistan located in the western highlands of the province between latitude 30°00 and 30°20 and longitude 66°50 and 67°15 in the form of landlocked watershed sub-basin (Fig. 1a). The intermountain synclinal basin stretches over an area of 1756 km^2, out of which 792 km^2 is covered by alluvium (Alam & Ahmad, 2014). The study was conducted in the capital city connecting with Afghanistan to its west. Topographically, Quetta is surrounded by high mountains namely Chilton, Takatu, and Murdar with altitudes ranging from 1000 to 4000 m. Climatic conditions are mostly arid consisting of long cold winters and short mild summers, receiving an average rainfall of ~ 100 mm/year (WAPDA, 2001).

The structural history of Quetta and its surroundings is quite complex due to massive folds and faults as it denotes the western edge of the collision zone between Indo-Pakistan and Eurasian plates, the collision consumed Tethys Ocean (Sagintayev et al., 2012). The study area (Quetta valley) contains geological formations from the recent Quaternary to Jurassic age (Fig. 1b). Quaternary deposits (Q) capping most of the basin comprises unconsolidated (sand, silt, and clay) to semi-consolidated (claystone, sandstone, and subordinate conglomerate overlying calcareous and carbonaceous beds) deposited because of weathering from the surrounding geological formation. Middle Jurassic (Jc), Chilton limestone light to dark grey, black, brownish to bluish grey, and in places with massive white limestone, fine-grained, oolitic, and reefoid, exposed in the east and west of the valley as outcrops that have contact with the highest thickness up to 1800 m found in the Quetta area. Lower Jurassic (Js) with the highest thickness up to1800 m is found in the Quetta area. Lower Jurassic (Js) contains grey to dark grey, thin- to medium-bedded coarse-grained shelly, oolitic, pesolitic, and pellitic limestone interbedded with shale and sandstone towards the base. Tertiary to Cretaceous (Tku) chocolate brown or dark grey limestone are exposed in the southeast and southwest with thickness ranging from 25 to 60 m. The lower tertiary Eocene marine shelf sequence (Tg) is composed of shale with interbedded sandstone and a marked thickness of 915 m at northeast. Upper Jurassic and cretaceous (Kjm) contain shale with interbedded limestone with an approximate thickness of 130 m but narrows towards Quetta (Kazmi et al., 2005; Sagintayev et al., 2012).

Hydrogeology and lithology

During the early twentieth century, Karezes and springs were the major irrigation sources (60%) in the upland areas of Baluchistan. At present in Quetta valley, groundwater is the only available source utilized by the inhabitants for agriculture, industrial, as well as domestic purposes. Due to overexploitation, the water table in the aquifer system of the Quetta Valley is declining at an alarming rate and groundwater is under great stress. From 1987 to 2013, groundwater decline ranged from 2.8 to 30.66 m in different areas of Quetta Valley (Durrani et al., 2018; Khair et al., 2015), with an average drop of 2.6 m/year in the overall area. Hydrogeologically, two types of aquifers exist in Quetta valley, namely, unconsolidated alluvial aquifer and hard bedrock aquifer. The majority of groundwater is extracted from the thick (30–900 m) alluvial deposits of Quaternary age (consisting of gravel, sand, and silt of different proportions) in the main valleys while less groundwater is extracted from the bedrock aquifers of Jurassic age (Kazmi et al., 2005). The aquifers are recharged from infiltration of precipitation runoff, inflow from the bedrock aquifer in the foothill areas, and in the surrounding mountain areas where these formations are exposed or hydraulically connected. The piedmont zone and stream beds are the main recharge zones, the gravel in these zones slope down towards the valley and are buried beneath the silt and loess which are 100–200 feet thick at some places. The rainwater infiltrates in basin piedmont and gravels to recharge aquifers in the central plain while moving so it encounters different lithological deposits. The rate of movement depends upon the size, arrangement of rock opening, gradient, and most important the lithological unit with which it comes into contact (Kazmi et al., 2005).

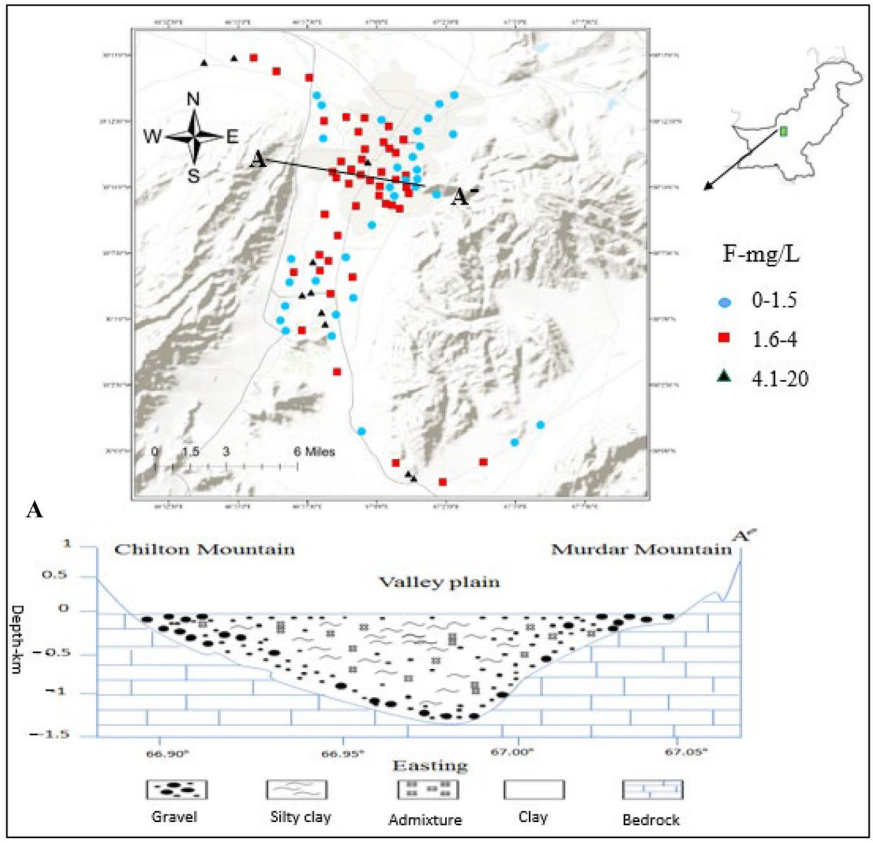

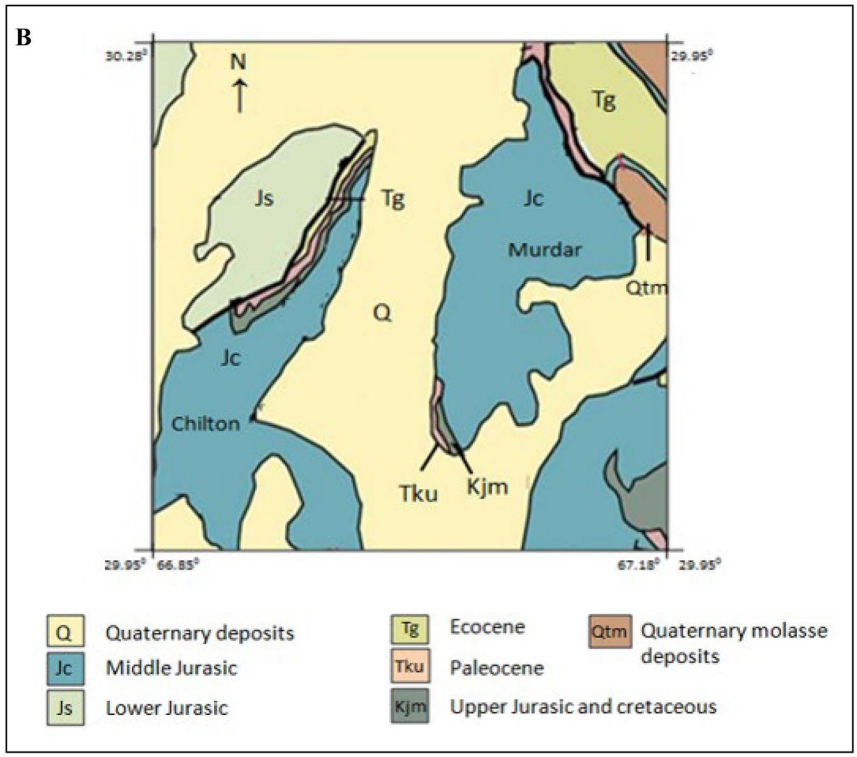

Fig. 1 **a** Location of the study area. Distribution of low (0–1.5 mg/L), high (1.6–4 mg/L), and very high (4.1–20 mg/L) groundwater fluoride in Quetta Valley along with schematic hydrological cross-section diagram. **b** Geological map of the study area

Materials and methods

Sampling and field analysis

A total of 87 groundwater samples from community tube wells and 5 composite surface soil samples were collected randomly from the sites where groundwater samples were collected to determine fluoride concentrations in different lithological units. Sampling was conducted in the first week of April 2016 along the path from where the major perennial rainwater stream generates from southeast to northwest. Before collection, groundwater was flushed for 10–15 min. EC, pH, and TDS were measured on-site by using multi-probe digital meter (HANNA) instruments that were already calibrated. Samples were collected in duplicates in 100 ml HDPE bottles for analysis of major cations and anions. All samples were stored at 4 °C before analysis following the sampling protocols as defined by APHA (2005). All samples were capped tightly and transported to the hydrogeochemistry lab of Quaid-i-Azam University, Islamabad for a detailed chemical analysis.

Laboratory analysis

Alkalinity was determined by titrating sample against hydrochloric acid (HCl). Chloride was determined by arganometric method while SO_4^{2-}, NO_3^{-}, and PO_4^{3-} were analyzed through UV–visible spectrophotometer (DR 5000) at wavelengths 420, 410, and 690 nm, respectively, following the standard protocol. For determination of major cations, groundwater was filtered through Whatman filter paper (No. 45) of 11 µm pore size, and pH was adjusted by adding 1–2 ml of ultrapure HNO_3. Major cations like (Ca^{2+}, Mg^{2+}, Na^{+}, and K^{+}) in groundwater samples were analyzed by a sequential Flame Photometer Atomic Absorption spectrophotometer (Varian Spectra AA-240) under standard operating conditions (APHA, 2005). Total hardness was calculated indirectly using the concentration of Ca^{2+} and Mg^{2+} by rearranging the following equation.

$$\text{Hardness} = \text{Mg}/0.243 + 2.5 \times \text{Ca}$$

Ion-selective electrode (ISE) was used to determine fluoride in groundwater and soil-using ISO-certified 9001-HANNA instrument; however, for water-soluble fluoride in soils, 5 g of soil and 25 ml distilled water were mixed in polyethylene bottles; the solution was centrifuged, and after allowing for 0.5 h, the resultant water was analyzed by the ion-selective electrode (HANNA). Simultaneously, EC and pH of soil samples were measured by making an aqueous solution at a ratio of 1:5 (soil and distilled water), the media was left overnight and then measured by using a multi-probe digital pH/EC meter (HANNA instruments) according to the standard protocols. Soil texture was determined by the hydrometer method while its mineralogical composition was found through X-ray diffraction spectroscopy using a standard protocol (APHA, 2005). To assure sample quality and integrity, essential quality control measurements were taken during sample collection and analyses. During the complete experimental process, all reagents used were certified and equipment soaked in 10% HNO_3 overnight.

Geochemical modeling of the mineral phases was assessed by pH redox equilibrium (PHREEQ) software. Saturation indices and Gibb's diagram were used for understanding hydrogeochemical processes. Statistical techniques were performed by using XLSTAT software; these include different multivariate analyses such as the correlation matrix and principal component analysis-multiple linear regression analysis (PCA-MLR) for interpretation of data sets. Study area map, concentration map, interpolation, and other geostatistical analyses were performed through ArcGIS 10.1.

Results and discussion

Major groundwater chemistry

Statistical summary of overall groundwater parameters with minimum, maximum, mean, and percentage of samples exceeding the WHO limit are listed in Table 1. According to the WHO, the pH of drinking water should be between 6.5 and 8.5; however, 9% of the samples exceeded the set limit. EC of the drinking water ranged from 321 to 2007 µS/cm, with 97% of the samples exceeding the WHO set limit of 400 µS/cm. In the study area, about 63% of the sample surpassed the threshold level for F^{-}. TDS is a measure of salinity, about 6% of the total samples have a TDS

Table 1 Statistical summary of groundwater physiochemical properties

Variables	WHO limit	Range	Mean ± SD	% > WHO limit
pH	6.5–8.5	7.1–8.9	8 ± 0.5	9
EC (μS/cm)	400	321.0–2007	779.2 ± 341.3	97
TDS (mg/L)	1000	215–1344.7	522.1 ± 228.5	6
F^- (mg/L)	1.5	0.0–20	2.8 ± 3.7	63
HCO_3^- (mg/L)	300	60.0–450	186.7 ± 88.5	10
Cl^- (mg/L)	250	4.0–547.8	90.8 ± 82.8	7
NO_3^- (mg/L)	50	9.1–23.5	10.6 ± 2.2	0
SO_4^{2-} (mg/L)	250	5.6–771.6	127.8 ± 116.6	8
PO_4^{3-} (mg/L)	0.1	−4.6–147.1	12.2 ± 26.8	69
Na^+ (mg/L)	200	5.8–70.6	48.6 ± 16.0	0
K^+ (mg/L)	30	−0.1–4.9	1.5 ± 0.8	0
Ca^{2+} (mg/L)	200	5.6–67.5	18.9 ± 9.6	0
Mg^{2+} (mg/L)	150	2.1–23.3	11.3 ± 5.9	0
Hardness (mg/L)	60–200	62–251	137 ± 45.04	–
Depth (m)	–	110.4–289.4	209.5 ± 45.1	–

Detection limits for PO_4^{3-} is 0.1 mg/L while for K it was 0.5 mg/L

Bdl below detection limit

value above the acceptable limit of 1000 mg/L. Na^+ and HCO_3^- in groundwater were marked as dominant cation and anions with concentrations of 70.6 and 450 mg/L, respectively. The national limit for fluoride in drinking water is 1.5 mg/L. In the overall groundwater samples, fluoride ranged between 0 and 20 mg/L. To sketch a clear view of the spatial distribution of groundwater fluoride, it was classified into three categories based on groundwater fluoride levels. First category contained low fluoride, i.e., 0–1.5 mg/L, second category contained high fluoride, i.e., 1.6–4.0 mg/L, and third category contained very high fluoride, i.e., 4.1–20 mg/L. The number of groundwater samples falling in low, high, and very high category was 37% ($n = 32$), 51% ($n = 44$), and 12% ($n = 11$), respectively. The ionic balances for all the groundwater samples were within the range − 1 to + 1, ensuring that the chemical analysis is suitable for further geochemical interpretation and processing.

To envisage and streamline the role of contributing variables on groundwater fluoride level, the concentrations of important variables were plotted against low, high, and very high groundwater F^- concentration in box plot to comprehend the dataset distribution of major variables as min, max, and median (Fig. 2). Among major controlling factors, EC, pH, Na, HCO_3, and Cl showed a linear trend with groundwater fluoride concentration while Ca, Mg, and depth showed a nonlinear trend with elevated concentration of groundwater fluoride. Furthermore, to know the interrelationship between F^- and the analyzed physicochemical variables, the correlation matrix (Pearson) was applied (Table S1). Correlation of cationic species with F^- in groundwater was found in the decreasing order as $K^+ > Na^+ > Mg^{2+} > Ca^{2+}$. Similarly, the correlation of F^- with anionic species was found in the decreasing order as $HCO_3^- > SO_4^{2-} > Cl^- > PO_4^{3-} > NO_3^-$. Correlation is based on high degree: if the coefficient value lies between ± 0.50 and ± 1, then it is said to be a strong correlation. Moderate degree: if the value lies between ± 0.30 and ± 0.49, then it is said to be a medium correlation. Low degree: when the value lies below ± 0.29, then it is said to be a small correlation. Among the overall physiochemical variables, HCO_3^- showed a high degree of positive correlation ($r^2 = 0.7$), potassium K^+ showed medium correlation ($r^2 = 0.3$) while (Ca^{2+}) on the other hand showed low correlation with F^- ($r^2 = -0.2$). Apart from all, a significant correlation of fluoride was seen with pH ($r^2 = 0.6$) which is recognized as an important parameter in the genesis of groundwater F^-.

Hydrogeochemistry of groundwater

Hydrogeochemistry of the area displayed a horizontal zonation from the mountain foot towards the basin plain. Groundwater quality degraded from the

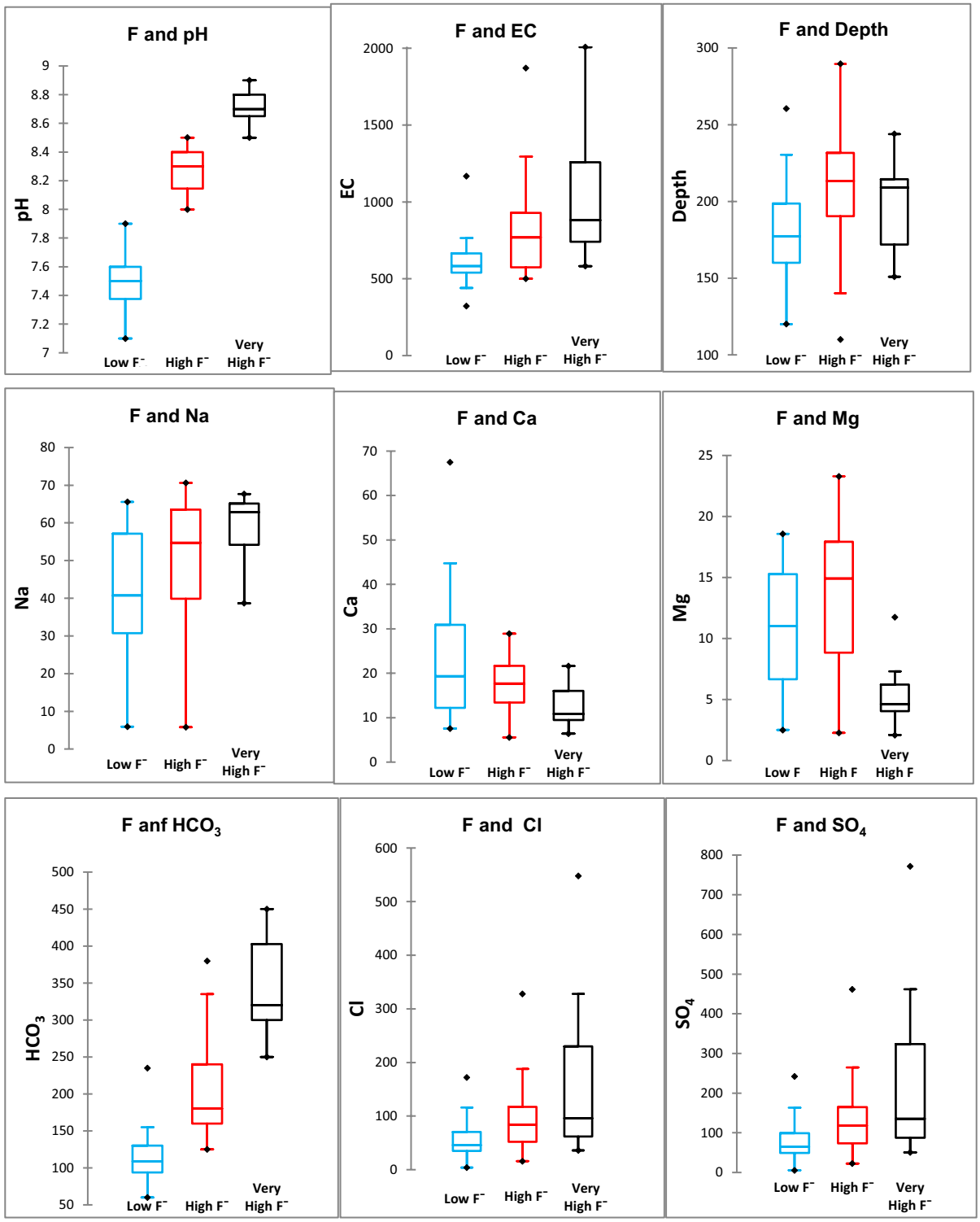

Fig. 2 Concentration of variables among low (0–1.5 mg/L), high (1.6–4 mg/L), and very high (4.1–20 mg/L) groundwater fluoride

mountainous recharge zone towards the central discharge zone. Hydro-chemical faces reflected chemical processes operative in a certain lithological environment and geochemical conditions. Chadha (1999) proposed a method for classification of water type in terms of different hydro-chemical faces by plotting the difference between $(CO_3^{2-} + HCO_3^{-})$ and $(Cl^{-} + SO_4^{2-})$ on the *x*-axis versus the difference between $(Ca^{2+} + Mg^{2+})$ and $(Na^{+} + K^{+})$ on *y*-axis expressed in meq/L in the form of Chadha diagram. The data plotted on the Chadha diagram (Fig. 3a) resulted in four different fields representing four different types of hydro-chemical faces, the plot helped us to understand the division of low and high fluoride groundwater types as well as the processes promoting their evolution. The decreasing order of water faces showed that percentage of $Na\text{-}HCO_3 > Ca\text{-}HCO_3 > Na\text{–}Cl > Ca\text{–}Mg\text{–}Cl$.

The predominant hydrogeochemical water type was found to be of $Ca\text{-}HCO_3$ in the recharge zone supported by low groundwater fluoride which may be due to the high recharge potential of piedmont zones and weathered products of the surrounding mountains such as carbonaceous rocks, representing hard water with $Ca\text{–}HCO_3$ faces while roughly the predominant water type was found to be of $Na\text{–}HCO_3$, Ca–Mg–Cl, and NaCl in the discharge areas of the basin plain, indicating slow movement and groundwater recharge. An increase in the concentration of HCO_3^{-} with F^{-} illustrated weathering of F^{-}-bearing minerals, supported by significant correlation ($r^2 = 0.7$). The most common source for Na^{+} in the groundwater was the dissolution of silicate minerals that showed a linear

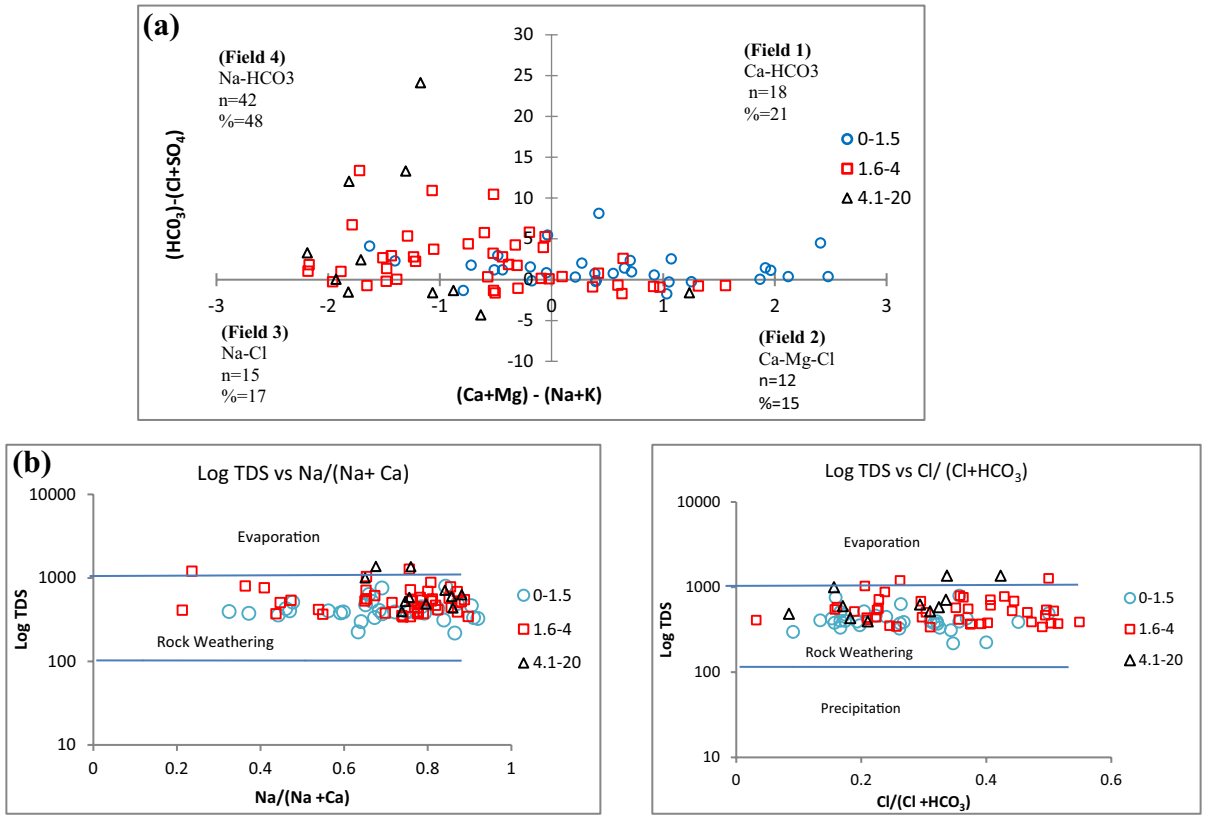

Fig. 3 **a** Chadha diagram showing classification of groundwater samples of the understudy area (Chadha, 1999). Field 1: $Ca\text{–}HCO_3$–type waters, reflecting recharge and weathering. Field 2: Ca–Mg–Cl–type waters, reflecting reverse ion exchange. Field 3: Na–Cl–type waters, reflecting evaporation or mixing. Field 4: $Na\text{–}HCO_3$–type waters, reflecting base ion exchange. **b** Gibb's plot indicating hydro-chemical processes for low (0–1.5 mg/L), high (1.6–4 mg/L), and very high (4.1–20 mg/L) groundwater fluoride

trend with HCO_3^- ($r^2 = 0.5$); this points that the long interaction time with the aquifer matrix and steady recharge of deep groundwater made conditions suitable for groundwater fluoride release. Similar results were seen by Rashid et al. (2020) with $CaHCO_3$ groundwater type to be associated with recharge processes and weathering while $NaHCO_3$ indicated base ion exchange.

To elaborate our discussion, major hydrogeochemical processes that influence groundwater chemistry was probed through Gibb's plot (Gibbs, 1970). The outcome of the result elucidated that majority of the samples fall in the rock weathering zone except for few high fluoride groundwater samples in which the evaporation process dominates (Fig. 3b), which further strengthens our discussion that weathering acted as a prominent process controlling the quality of groundwater of the valley as compared with other processes. For sketching the view of cation-exchange processes and scenarios within the aquifer-hosting geological unit, chloro-alkaline indices (CAI) was used, which was calculated using the following equations:

$$\mathrm{CAI1} = (\mathrm{Cl} - (\mathrm{Na} + \mathrm{K})/\mathrm{Cl})$$

$$\mathrm{CAI2} = (\mathrm{Cl} - (\mathrm{Na} + \mathrm{K}))/(\mathrm{SO_4} + \mathrm{HCO_3} + \mathrm{NO_3})$$

Positive values of both CAI 1 and CAI 2 mean that dissolved Na^+ and K^+ in the water solution were exchanging with the Mg^{2+} and Ca^{2+} of the clay or rock matrix (Fig. 4). In turn, if the exchange occurred in the reverse order, then the chloro-alkaline indices should be negative. The greater the value of both indices, the more significant is the impact of cation exchange in groundwater. This exchange process can be represented as.

$$2\mathrm{Na{-}clay/rock} + (\mathrm{Mg^{2+}} + \mathrm{Ca^{2+}}) - \mathrm{water} \ll -- \gg (\mathrm{Ca^{2+}} + \mathrm{Mg^{2+}}) - \mathrm{clay/rock} + 2\mathrm{Na} - \mathrm{water}$$

CAI indices of groundwater vary from − 15.3 to 3.4 and − 15.3 to 4.5 for CAI 1 and CAI 2, respectively. Figure 4 shows that all the groundwater in the study area was influenced by the cation exchange process, where Na^+ and K^+ of the aquifer matrix that contained clay minerals were exchanging with Mg^{2+} and Ca^{2+} in the groundwater. During the ion-exchange process, Mg^{2+} and Ca^{2+} precipitate; it occurs when Na^+ in the groundwater dominates allowing its exchange with F^- on clay minerals and hence the mobility of groundwater fluoride (Rashid et al., 2020). The products of secondary weathering such as kaolinite and smectite as well as marine (fine-grained oolite, reefoid, shale) and non-marine sediment sequence in the study area provided abundant exchange sites to facilitate this process. Moreover, the stagnant nature of groundwater in the valley plain and longer residence time made conditions favorable for the promotion of the cation exchange process (Hossain et al., 2016; Rashid et al., 2018).

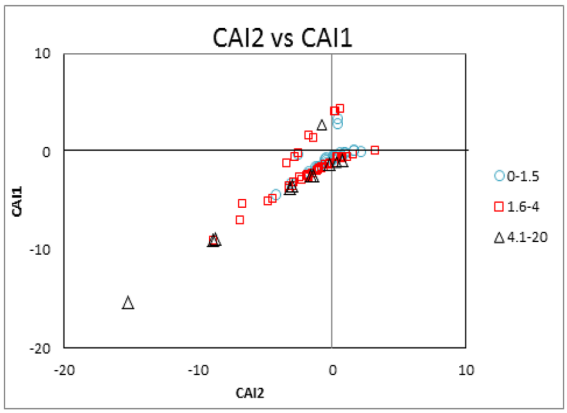

Fig. 4 Scatter plot of CAI1and CAI2 for low (0–1.5 mg/L), high (1.6–4 mg/L), and very high (4.1–20 mg/L) groundwater fluoride samples

Distribution of low and high groundwater F^-

The valley filled unconsolidated to semi-unconsolidated recent deposits influenced the water quality, especially groundwater F^- concentration in the study area (Fig. 1a). According to Kazmi et al. (2005), these deposits showed a great variation from the mountain towards the central basin. The mountain foot with piedmont characteristics contains enormous, small- to large-sized gravels; however, moving towards the central plain, the gravels are buried beneath silt and loess of insignificant depth, they are hydraulically connected with the gravels of the piedmont zone.

Low and high groundwater F^- showed horizontal zonation in the synclinal Quetta valley from the mountain towards the central plain. Low groundwater F^- mostly occurred near the foot of massive limestone mountains (Jurassic age) in the east and west of the study area as highlighted with circles compared to high groundwater F^- that was found in central valley with recent Quaternary deposits of secondary weathered products (sand, silt, and clay) in the northwest and south of the valley. In the northwest middle, Jurassic units as outcrops with sandstone and shale having fluoride content of 270 and 740 mg/L, respectively, may give rise to high groundwater F^-. While on the south of the valley, Paleocene units as outcrops with shale and interbedded limestone were found giving rise to very high groundwater F^- (Wen et al., 2013). This can be seen in Fig. 1b where groundwater fluoride levels are related to geological units. In the center of the basins, quaternary aquifers mostly contained high levels of groundwater fluoride; this may be due to slow recharge from adjacent groundwater channels providing high residence time for interaction between aquifer matrix and groundwater favoring abnormal level of groundwater F^- (Fig. 5). It is supported by hydraulic conductivity that generally transformed from 40 to 20 mm/h moving from high-altitude area to comparatively low-altitude area of the basin (Khair et al., 2015). Major cations such as Ca^{2+} and Mg^{2+} showed low and moderate negative correlation with groundwater F^- ($r^2 = -0.2$, $r^2 = -0.3$), respectively, and envisaged clear distinction when plotted against the groundwater flow that is from mountain foot towards the valley (Table S1; Fig. 5b, c). As we moved from the mountains towards the central plain, the concentration of such ions decreased, favoring the genesis of high to very high groundwater F^- (Fig. 5a). A negative correlation of fluoride with Ca^{2+} in groundwater had been observed by several studies around the world (Mao et al., 2021; Mukherjee et al., 2015; Rashid et al., 2020). The possible sources of these divalent cations may be due to the interaction of groundwater with associated minerals such as calcite, feldspar, dolomite, serpentine, etc.

Ion concentration of Na^+/Ca^{2+} ratio when plotted against the groundwater flow showed a slight increase with F^- concentration (Fig. 5g); this may be due to common ion effect that replaces Ca^{2+} ion with Na^+ ion, representing the cation-exchange-rich sites of the clayey matrix which may be mobilizing free F^- in groundwater. Among the monovalent ions, K^+ showed moderate correlation with F^- ($r^2 = 0.3$), which may originate from the dissolution of associated minerals (e.g., potash-feldspar, illite, fluorapatite, and mica) associated with clay to silt clay units and was responsible for high concentration as groundwater flow converges to discharge. Electrical conductivity which is a measure of dissolved salts increased along the groundwater flow path indicating that as we moved towards the basin, the freshwater turned to become more saturated with dissolved salts and subsequently the ionic strength, which helped in the enrichment of groundwater F^- due to steady-state circulation of groundwater. Among major anions, HCO_3^- with a highly significant correlation of ($r^2 = 0.8$), behaved as releasing factor for the mobility of fluoride through the dissolution of F^--bearing minerals and can be illustrated by the following reaction (Eq. 1).

$$CaF_2 + 2HCO_3 = CaCO_3 + 2F^- + H_2O + CO_2 \quad (1)$$

The above stoichiometric equation tells that the greater the HCO_3^- level in groundwater, the more will be the dissolution of fluorite (CaF_2) mineral, as two moles of bicarbonate are required for the dissolution of 1 mol of fluorite in groundwater and hence releasing 2 mol of free fluoride ions. Saxena and Ahmed (2001) put forth that alkaline conditions with pH ranging between 7.6 and 8.6 are favorable for the dissolution of fluorite minerals from the host rocks. At $pH \leq 6$ F^- is mostly found attached on the clay surfaces, an increase in pH causes the replacement of F^- from the clay minerals with OH^- ion in the water of typically similar radius under anionic exchange process as explained below.

Muscovite: $KAl_2\ [AlSi_3O_{10}]F_2 + 2OH^- = KAl_2[AlSi_3O_{10}][OH]_2 + 2\ F^-$
Biotite: $KMg_3[AlSi_3O_{10}]F_2 + 2OH^- = KAl_2[AlSi_3O_{10}][OH]_2 + 2\ F^-$
Fluorite: $CaF_2 + 2OH^- = Ca\ (OH)_2 + 2\ F^-$

The plot of pH when plotted against the groundwater flow and subsequently fluoride concentration showed significant relation ($r^2 = 0.6$), indicating that the mobility of fluoride is driven from the dissolution of F^--bearing minerals and dissociation from active sites of abundant clay minerals (Fig. 5h),

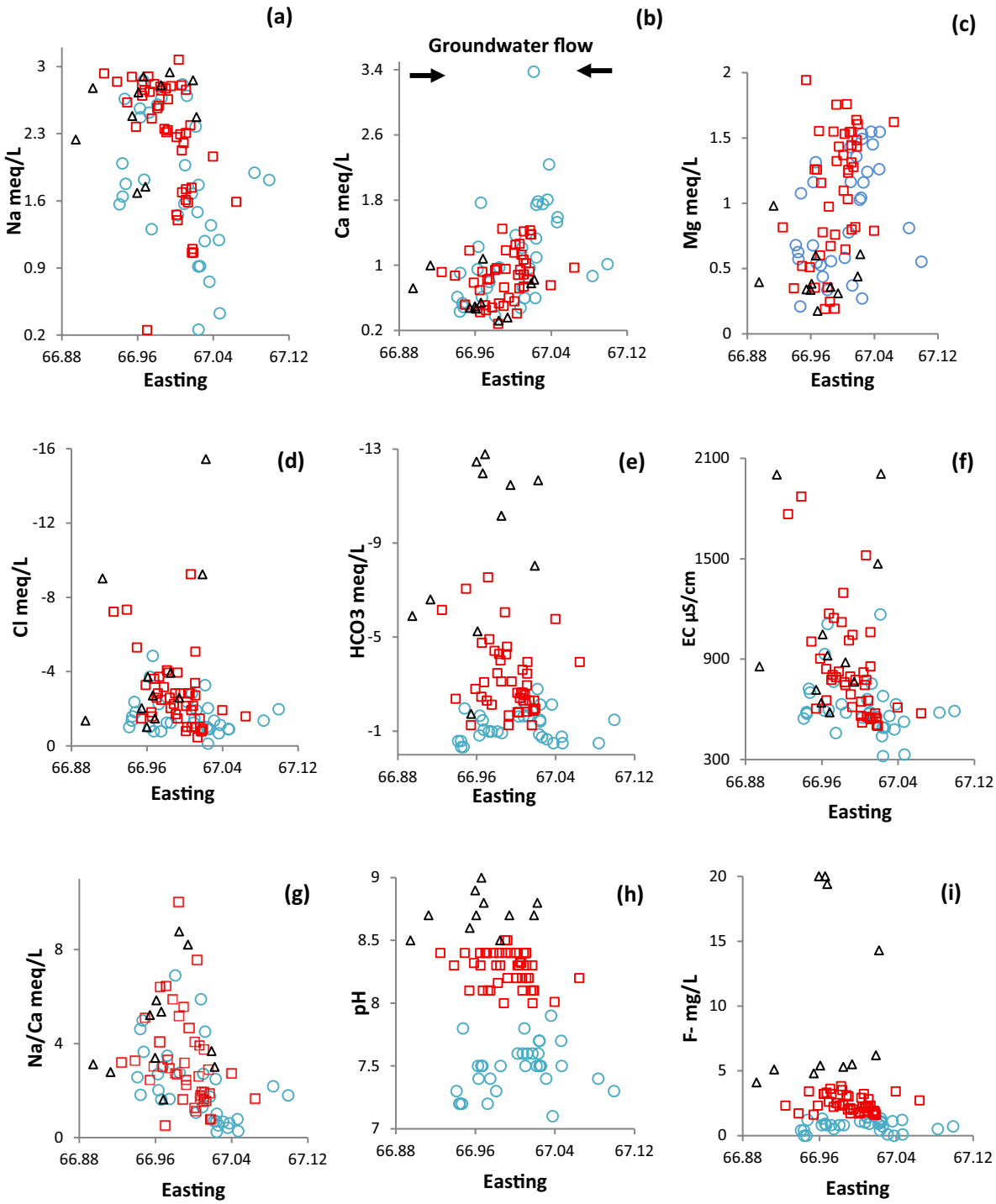

Fig. 5 Ion concentration of groundwater versus longitude plots **a** Na, **b** Ca, **c** Mg, **d** Cl, **e** HCO_3, **f** EC, **g** Na/Ca, **h** pH, and **i** F. Legends for groundwater samples: empty blue circles, 0–1.5; empty red squares, 1.6–4; and empty black triangles, 4.1–20 mg/L

similar relations have been seen by Hossain et al. (2016) (Table S1).

F^- concentration and control of lithology

Several studies have been conducted so far on the depth-dependent variability of fluoride in groundwater of different basins such as the Taiyuan basin, Zhangye basin, Datong basin, and Yuncheng basin (Hu et al., 2016; Luo et al., 2018; Pi et al., 2015; Wen et al., 2013). In such basins, groundwater with shallow depth seemed to have elevated fluoride concentration with evaporation process acting as a driving force causing precipitation of calcite, due to which groundwater becomes deficit with Ca^{2+} making conditions favorable for dissolution of F^--bearing minerals (CaF_2), while high-depth groundwater was uncontaminated in terms of F^- concentration. However, in the study area (Quetta Valley), upper high-altitude groundwater found at depth < 170 m is observed to be least contaminated as compared to lower, low-altitude groundwater with depth > 170 m, when plotted against the depth, groundwater flow, and subsequently groundwater fluoride levels (Fig. 6). Few high groundwater F^- samples are obtained from upper groundwater of 170 m; these samples are obtained from the northwest (middle Jurassic) and south (Pliocene) with shale as a common unit. From the plot, low groundwater fluoride was hosted at the edges of the basin with high altitude as compared to the low-altitude central basin.

Upper high-altitude groundwater was found to be associated with low EC, low HCO_3^-, and low Na^+ but high in terms of Ca^{2+}, whereas on the other hand, the low-altitude groundwater at depth up to 300 m is linked to comparatively high EC, high HCO_3^-, high Na^+, and low Ca^{2+}. The groundwater of the study area, geographically lying in an arid zone is least affected by evaporation because even the upper groundwater at depth < 170 m is rich in Ca^{2+}, while high evaporation causes the precipitation of Ca^{2+} in the form of various minerals.

The study area once known for its karez system and shallow groundwater found at depth up to 30 m have turned into deep aquifers with water table declining up to 10 m/year due to uncontrolled groundwater abstraction (Khair et al., 2015). Abstraction of lower-depth groundwater with heterogenic lithology especially increases in thickness of silty clay towards the center caused the evolution of high fluoride groundwater; such groundwater is frequently observed at the valley plain supported by high Na^+, high K^+, and high HCO_3^- that may be associated with the dissolution and hydrolysis of silicate minerals such as silty clay and clay matrices. A similar finding was reported by Pi et al. (2015). High groundwater F^- is further dependent on factors such as the preferential pathways followed by the groundwater recharge, residence time, well depth, circulation within different lithological units, and the hydrological conditions.

Groundwater fluoride concentrations were compared with the well logs of the basin and its subsequent lithological units (Fig. S1). It clearly illustrated the control of geomorphological units on groundwater quality especially in terms of groundwater F^- concentration. Wells 1 and 2 were taken from the recharge zones of west and east at depths of 120 and 130 m of the valley showing a comparatively low concentration of F^- 0.1 and 1.1 mg/L, respectively, with greater thickness of admixture and gravel units compared to wells 3 and 4 that were taken from the discharge zones at depths of 200 and 230 m in the basin plain with F^- concentration of 2 and 3.3 mg/L and having a greater thickness of silty clay and clay units. When related with the surface soil, the soil collected mostly from the mountain foot appeared to be of sandy loamy texture with soluble F^- ranging from 0.01 to 1 as compared to the soluble fluoride content in silty soil of central valley with soluble F^- ranging from 0 to 2.3. According to Farooqi et al. (2009), the mean soluble F^- in subsurface silty soil-30 cm (1.9 mg/kg) > surface sandy soil-0 cm (0.8 mg/kg). However, the highest soluble F^- up to 2.3 mg/L in the study area was evidenced in soil with clayey loam texture, a high value of EC 1700, and alkaline pH 8 (Table S2).

High F^- concentration in such wells may be linked to an increase in the depth of silty clay and clay units as compared to their depth in low F^- wells. An increase in F^- concentration due to the thickness of fine sediments has also been reported in several studies. F^- occurs within clay minerals or adsorbed to it. Activity and sorption capacity of sand < silt << clay (Calvi et al., 2016; Wen et al., 2013). According to Liu et al. (2015), F^- in sediments ranged from 140 to 1690 mg/kg; however, F^- content in clay to silty clay > silty-fine sand > fine sand > coarse sand. Another possible reason that may be linked to the low and

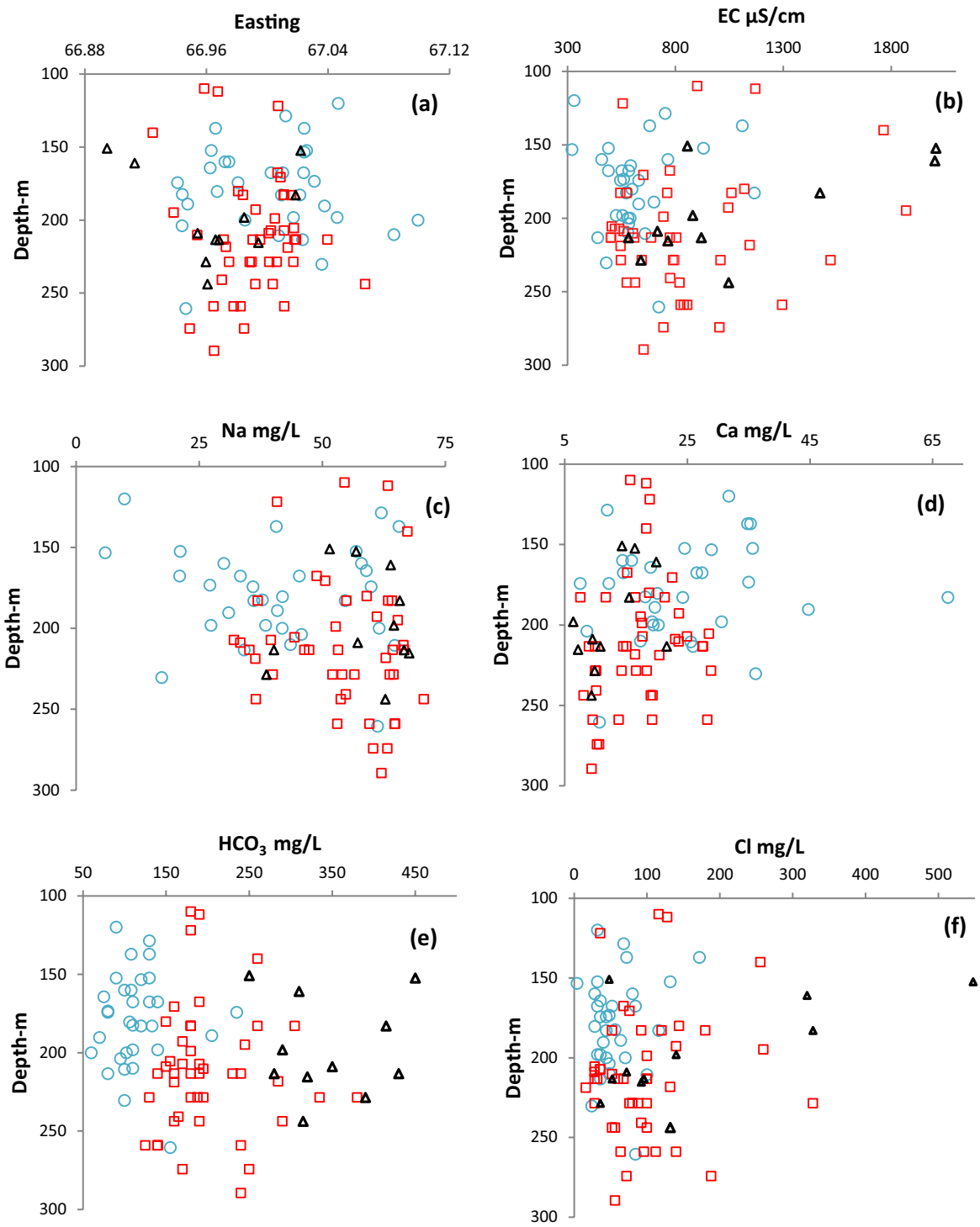

Fig. 6 Depth-dependent relation of F^- with **a** longitude, **b** EC, **c** Na, **d** Ca, **e** HCO_3, and **f** Cl. Legends for groundwater samples: empty blue circles, 0–1.5; empty red squares, 1.6–4; and empty black triangles, 4.1–20 mg/L, respectively

high F^- groundwater is the lateral recharge of the groundwater in the central plain from the mountain foot giving a maximum time for the interaction between steady flow groundwater and fluoride-rich aquifer matrix; hence, we encountered an abnormal level of groundwater F^-.

Geochemical modeling was used by calculating the saturation indices (SI) and predicting the reactive mineralogy of the subsurface from groundwater data without collecting the samples of the solid phase and analyzing its mineralogy. If the mineral has saturation indices SI = 0, the groundwater sample is said to be saturated with that mineral, if the mineral has SI > 0, the groundwater is supersaturated reflecting precipitation is required to attain equilibrium, and if SI < 0, the groundwater is said to be undersaturated which means further dissolution is required to reach equilibrium. Geochemical factors in terms of saturation indices of different minerals (fluorite, calcite, halite, and gypsum) are shown in Figs. S2a and S2b. The mean SI of different minerals was found in the decreasing trend as calcite ($CaCO_3$) > fluorite (CaF_2) > gypsum ($CaSO_4{\cdot}2H_20$) > halite (NaCl). Among all minerals, mineral calcite ($CaCO_3$) is important because it shares common ion (Ca^{2+}) with fluorite (CaF_2) and controls the dissolution of groundwater fluoride. Fluoride concentrations in groundwater are restricted by fluorite solubility, i.e., in the presence of 40 mg/L calcium, it should be restricted to 3.1 mg/L (Fawell & Bailey, 2006). The calculation of saturation indices for calcite and fluorite is plotted in Fig. S2b.

All the groundwater samples were in the saturation phase for calcite, while for halite minerals, all the samples were undersaturated which means more minerals can dissolve in the groundwater. Fluoride seemed to be undersaturated with fluorite except for few very high groundwater F^- samples that were in oversaturated phase. This further supports our hypothesis that neither the dissolution of fluorite (CaF_2) nor the precipitation of calcite ($CaCO_3$) seemed to be the mechanism controlling the concentration of F^-, as reported by many studies (Edmunds & Smedley, 2013). Fluoride, as a strong ligand in water, may form soluble complexes with polyvalent cations, such as, Mg^{2+}, Al^{3+}, and Ca^{2+} depending upon the water pH, while its mobility in groundwater is attributed to desorption from metal oxides present in the loess sediments that compose the aquifer (Currell et al., 2011).

Mineral composition of soil

The distribution of soluble fluoride in the soil of the study area along with the mineralogy and physicochemical parameters (EC, pH, and texture) of the 5 soil samples are listed in Table S2. The accumulation of F^- is based on fluoride-bearing minerals in the soil. The overall soluble F^- content in the soil showed a positive correlation with EC and pH. Generally, pH acts as a governing factor for the leaching of F^- from soil and subsequent enrichment of F^- in the aquifers. Clayey soil tends to adsorb F^- on the surface at pH < 6 and tends to desorb it at pH above 6. The soil of the study area is calcrete in nature; calcretes and dolocretes are found to contain F^- to a maximum of 1%. The average abundance of F^- in the soil is 100–300 mg/kg. However, hardly 5–10% of the total soil F^- content is water soluble. Chemical analysis of calcrete samples from Nalgonda District of India observed F^- content in the range of 440–1160 mg/kg (Reddy et al., 2016). The percentage weightage for important minerals that played a vital role in groundwater mobility is listed in Table S2.

In general, F^- in the earth's crust is present in different forms and associated with different minerals like silicates (e.g., humite $(MgFe)7(SiO_4)_3(F,OH)_2$; topaz $Al_2SiO_4(F,OH)_2$)), phosphates (e.g., wagnerite $(MgFe)2PO_4F$; apatite $Ca5(PO_4)_3$ (FClOH); amblygonite $(LiNa)AlPO_4(F,OH)$); calcium (e.g., fluorite CaF_2; fluorapatite $Ca5(PO_4)3F$); magnesium (e.g., sellaite, MgF_2), etc. are the chief sources of fluoride in groundwater (Farooqi et al., 2009). From the result of the mineral phase identification (Fig. S3) through the XRD diffraction pattern of soil, we found that the percentage of fluorite mineral in samples S1 and S2 collected near the foot of the mountains with sandy loamy texture was 2% and 3.7% as compared to the soil samples S3, S4, and S5 collected from the central valley with clayey loam texture having fluorite content of 6.5%, 7.7%, and 2.8%. Many minerals contain F^- as a primary constituent or as an impurity. Among primary minerals, biotite and muscovite contain about 1 wt.% of F^-, while fluoride contents are higher in accessory minerals, such as fluorapatite (~3.8 wt.%), topaz (~11.5 wt.%), and fluorite (~48 wt.%) (Edmunds & Smedley, 2013). The soil samples of the central valley were found to have high concentrations of fluorite mineral as compared to those collected from the mountain foot and can be found in

Table 2 Principal component analysis

Principal component matrix				
Variables	Component			
	PC1	PC2	PC3	PC4
Depth	−0.265	−0.131	**0.736**	**0.235**
pH	0.356	**0.762**	−0.086	**0.206**
EC	**0.938**	0.139	−0.075	−0.076
F^-	0.167	**0.877**	0.014	0.102
HCO_3^-	**0.554**	**0.718**	0.066	0.107
Cl^-	**0.936**	0.135	−0.072	−0.090
NO_3^-	0.167	−0.111	−0.118	**0.554**
SO_4^-	**0.936**	0.135	−0.072	−0.090
PO_4	0.063	−0.088	**0.638**	**0.331**
Na	**0.624**	0.195	0.334	−0.131
K	**0.613**	0.161	0.256	**0.378**
Ca	0.135	−0.382	**−0.645**	0.125
Mg	0.178	0.306	**−0.571**	**0.517**
Eigenvalue	4.943	2.115	1.404	1.228
% of variance	35.307	15.106	10.027	8.768
% of cumulative	35.307	50.413	60.44	70.012

Values in bold are different from 0 with a significance level alpha=0.05

good relationship with high concentrations of groundwater fluoride levels in the central basin.

Principal component analysis

For defining the meaningful role of major variables on groundwater fluoride chemistry, multivariate statistical analysis (PCA-principal component analysis) was performed on 13 major variables analyzed in 87 groundwater samples up to 4 principal components (PCs), which explained 70% of the total cumulative variance (Table 2).

Loading of variables in four components expressed the correlation between major variables in each component. In terms of hydrochemical applications, PCs can be interpreted to determine processes governing groundwater chemistry such as water–rock interactions, desorption, evaporation, ion-exchange processes, and anthropogenic inputs by examining loadings of variables in each of the PC; PC-1 showed 35% variance with highest eigenvalue of 4.94 and positive loading of EC, Na, K, SO_4, Cl, HCO_3, Ca, and Mg with coefficient correlation (r^2) of 0.938, 0.624, 0.613 0.936, 0.936, 0.554, 0.135, and 0.178, respectively, illustrating the general chemistry of groundwater due to water–rock interaction and mineral weathering in a sedimentary basin with complex geological formation ranging from recent Quaternary to Jurassic age formations. PC-2 showed 15.10% of the variance with an eigenvalue of 2.12 and positive loading of F^- with pH, and HCO_3^- with coefficient correlation (r^2) of 0.762, 0.877, and 0.718, respectively, described that dissolution of fluoride-bearing minerals during water–rock interactions, desorption of fluoride from secondary silicate minerals (muscovite, biotite, apatite, illite, smectites, fluorite, and shale), active organic surfaces and especially ion-exchange processes between F^- and OH^- in alkaline conditions were driving the fluoride concentration in groundwater (Luo et al., 2018; Rashid et al., 2020). PC-3 shows 10% variance with eigenvalue of 1.40, high positive loading of depth in PO_4^{3-}, Na^+, and K^+, and negative loading of Ca^{2+}, Mg^{2+}, and Cl^- with coefficient correlation (r^2) of 0.736, 0.638, 0.334, 0.246, −0.645, −0.571, and −0.072, respectively, denoting the biogeochemical weathering of Eocene age marine sequences (oolitic, pesolitic, pellitic, and reefoid limestone) interbedded with shale and sandstone towards the base in deep groundwater contributed to high loading of PO_4^{3-} with depth indicating another insight of F^- release by acting as a competing sorbent ion (Gao et al., 2013). Whereas moderate to low loading of Na^+ and K^+ showed inverse relation with Ca^{2+}, Mg^{2+}, and Cl^-, indicating reverse base ion-exchange processes with the silicate mineral. PC-4 contributed 8.76% variance with an eigenvalue of 1.21, moderate loading of nitrate and magnesium, low loading of depth, pH, PO_4^{3-}, K^+, and Ca^{2+} with coefficient correlation (r^2) of 0.554, 0.517, 0.235, 0.206, 0.331, 0.378, and 0.121, respectively; moderate loading of NO_3^- depicts that the groundwater may be affected by human inputs from domestic wastewater discharges and septic tank leakage due to diffuse recharge and extensive groundwater mining in quaternary aquifers; the positive loading of most variables in this component indicated a mixture of both natural and anthropogenic processes. However, this does not coincide with the high loading of EC (Jehan et al., 2019; Mao et al., 2021; Rashid et al., 2018). The overall processes indicate the effect of lithological influences on the enrichment of groundwater solutes especially fluoride in the sedimentary basin, Quetta Valley.

Conclusions

The study examined the spatial distribution of groundwater fluoride with the lithogeochemical approach.

- High groundwater F^- concentrations were evidenced in the synclinal basin while low groundwater F^- concentrations were found near the mountains' foot.
- High groundwater F^- was supported by Na-HCO_3 groundwater-type water with high HCO_3^- and high Na/Ca, indicating the influence of cation exchange on fluoride enrichment and mobilization.
- Fluorite was undersaturated in most of the samples indicating groundwater F^- does not come from the dissolution of the mineral fluorite nor its precipitation has any role.
- All the samples were influenced by rock-weathering processes, indicating the dominance of the hydrological process while the genesis of fluoride is related to the F^--bearing silicate mineral.
- PCA revealed that alkaline pH and the presence of competitors to sorption (especially HCO_3, OH) facilitate F^- mobilization, especially in such basins where immense pumping and water table drawdown have caused the mixing of heterogeneous lithological units (sandstone, silty clay, and clay sediments) giving rise to high groundwater F^-.
- Due to complex geological features, F^- enrichment in groundwater sedimentary basin Quetta is affected by a broad-scale process across a wide area, depths, hydraulic conductivity, residence times, and most importantly the geomorphological units hosting the aquifer matrix.
- Abnormal levels of F^- in groundwater are of great concern to the public health in Quetta; therefore, continuous monitoring of groundwater fluoride and its management is recommended.

Acknowledgements The study was financially supported by the Department of Environmental Science, Quaid-i-Azam University, Islamabad. Sir Mazhar and Sir Abdullah of Public Health and Engineering Department (PHED) Quetta shared valuable data of the well logs, while Dr. Yaqoob of the National Center of Physics (NCP) helped in soil analysis; without their support and assistance, the study would have been impossible to be conducted.

Data availability Data analyzed during this study can be found in this manuscript and supplementary information file.

References

Ainsworth, N. (1933). Mottled teeth. *British Dental Journal, 55*, 233–250.

Alam, K., & Ahmad, N. (2014). Determination of aquifer geometry through geophysical methods: A case study from Quetta Valley Pakistan. *Acta Geophysica*. https://doi.org/10.2478/s11600-013-0171-8

APHA (2005): *Standard Methods for the Examination of Water and Wastewater*. American Public Health Association

Azizullah, A., Khattak, M. N., Richter, P., & Hader, D. P. (2011). Water pollution in Pakistan and its impact on public health–a review. *Environmental International, 37*(2), 479–497. https://doi.org/10.1016/j.envint.2010.10.007

Brindha, K., and Elango, L. (2011). Fluoride in groundwater: causes, implications and mitigation measures. *Fluoride properties, applications, and environmental management*, 111–136.

Calvi, C., Martinez, D., Dapeña, C., & Gutheim, F. (2016). Abundance and distribution of fluoride concentrations in groundwater: La Ballenera catchment, southeast of Buenos Aires Province Argentina. *Environmental Earth Sciences, 75*(6), 1–12. https://doi.org/10.1007/s12665-015-4972-8

Chadha, D. (1999). A proposed new diagram for geochemical classification of natural waters and interpretation of chemical data. *Hydrogeology Journal, 7,* 431–439.

Chae, G. T., Yun, S. T., Mayer, B., Kim, K. H., Kim, S. Y., Kwon, J. S., & Koh, Y. K. (2007). Fluorine geochemistry in bedrock groundwater of South Korea. *Science of the Total Environment, 385*(1–3), 272–283. https://doi.org/10.1016/j.scitotenv.2007.06.038

Chandio, T. A., Khan, M. N., & Sarwar, A. (2015). Fluoride estimation and its correlation with other physicochemical parameters in drinking water of some areas of Balochistan Pakistan. *Environmental Monitoring and Assessment, 187*(8), 1–9. https://doi.org/10.1007/s10661-015-4753-6

Chen, H., Yan, M., Yang, X., Chen, Z., Wang, G., Schmidt-Vogt, D., & Xu, J. (2012). Spatial distribution and temporal variation of high fluoride contents in groundwater and prevalence of fluorosis in humans in Yuanmou County, Southwest China. *Journal of Hazardous Mater, 235*, 201–209. https://doi.org/10.1016/j.jhazmat.2012.07.042

Currell, M., Cartwright, I., Raveggi, M., & Han, D. (2011). Controls on elevated fluoride and arsenic concentrations in groundwater from the Yuncheng Basin China. *Applied Geochemistry, 26*(4), 540–552. https://doi.org/10.1016/j.apgeochem.2011.01.012

Dean, H. T., & Elvove, E. (1937). Further studies on the minimal threshold of chronic endemic dental fluorosis. *Public Health Reports, 1896–1970*, 1249–1264.

Durrani, I. H., Adnan, S., Ahmad, M., Khair, S. M., & Kakar, E. (2018). Observed long-term climatic variability and its impacts on the groundwater level of Quetta alluvial. *Iranian Journal of Science and Technology Transactions A Science, 42*(2), 589–600. https://doi.org/10.1007/s40995-017-0235-8

Edmunds, W. M., and Smedley, P. L. (2013). Fluoride in natural waters *Essentials of medical geology* (pp. 311–336): Springer, Dordrecht.

Farooqi, A., Masuda, H., Siddiqui, R., & Naseem, M. (2009). Sources of arsenic and fluoride in highly contaminated soils causing groundwater contamination in Punjab, Pakistan. *Archives of Environmental Contamination and Toxicology, 56*(4), 693–706. https://doi.org/10.1007/s00244-008-9239-x

Fawell, J. K., and Bailey, K. (2006). *Fluoride in drinking-water*. World Health Organization

Gao, X., Su, C., Wang, Y., & Hu, Q. (2013). Mobility of arsenic in aquifer sediments at Datong Basin, northern China: Effect of bicarbonate and phosphate. *Journal of Geochemical Exploration, 135*, 93–103. https://doi.org/10.1016/j.gexplo.2012.09.001

Gibbs, R. J. (1970). Mechanisms controlling world water chemistry. *Science, 170*(3962), 1088–1090.

He, X., Li, P., Wu, J., Wei, M., Ren, X., & Wang, D. (2021). Poor groundwater quality and high potential health risks in the Datong Basin, northern China: Research from published data. *Environmental Geochemistry and Health, 43*(2), 791–812. https://doi.org/10.1007/s10653-020-00520-7

Hossain, M., & Patra, P. K. (2020). Hydrogeochemical characterization and health hazards of fluoride enriched groundwater in diverse aquifer types. *Environmental Pollution, 258*, 113646. https://doi.org/10.1016/j.envpol.2019.113646

Hossain, S., Hosono, T., Yang, H., & Shimada, J. (2016). Geochemical processes controlling fluoride enrichment in groundwater at the western part of Kumamoto area, Japan. *Water Air Soil Pollution, 227*(10), 1–14. https://doi.org/10.1007/s11270-016-3089-3

Hu, Y., Xia, C., Dong, Z., & Liu, G. (2016). Geochemical characterization of fluoride in the groundwater of the Huaibei Plain China. *Analytical Letters*. https://doi.org/10.1080/00032719.2016.1199027

Hu, Y., You, M., Liu, G., & Dong, Z. (2021). Spatial distribution and potential health risk of fluoride in drinking groundwater sources of Huaibei, Anhui Province. *Scientific Reports, 11*(1), 1–11. https://doi.org/10.1038/s41598-021-87699-6

Jadhav, S. V., Bringas, E., Yadav, G. D., Rathod, V. K., Ortiz, I., & Marathe, K. V. (2015). Arsenic and fluoride contaminated groundwaters: A review of current technologies for contaminants removal. *Journal of Environmental Management, 162*, 306–325. https://doi.org/10.1016/j.jenvman.2015.07.020

Jehan, S., Khan, S., Khattak, S. A., Muhammad, S., Rashid, A., & Muhammad, N. (2019). Hydrochemical properties of drinking water and their sources apportionment of pollution in Bajaur agency, Pakistan. *Measurement, 139*, 249–257. https://doi.org/10.1016/j.measurement.2019.02.090

Kazmi, A., Abbas, G., Younas, S. (2005). Water resources and hydrogeology of Quetta Basin, Balochistan, Pakistan. Geological Survey of Pakistan, Quetta

Khair, S. M., Mushtaq, S., & Reardon-Smith, K. (2015). Groundwater governance in a water starved country: Public policy, farmers' perceptions, and drivers of tube well adoption in Balochistan. *Pakistan. Ground Water, 53*(4), 626–637. https://doi.org/10.1111/gwat.12250

Kim, K., & Jeong, G. Y. (2005). Factors influencing the natural occurrence of fluoride-rich 711 groundwaters: A case study in the southeastern part of the Korean Peninsula. *Chemosphere, 58*(10), 1399–1408.

Liu, H., Guo, H., Yang, L., Wu, L., Li, F., Li, S., & Liang, X. (2015). Occurrence and formation of high fluoride groundwater in the Hengshui area of the North China Plain. *Environmental Earth Sciences, 74*(3), 2329–2340.

Luo, W., Gao, X., & Zhang, X. (2018). Geochemical processes controlling the groundwater chemistry and fluoride contamination in the Yuncheng Basin, China—An area with complex hydrogeochemical conditions. *PLoS ONE, 13*(7), e0199082. https://doi.org/10.1371/journal.pone.0199082

Mao, M., Wang, X., & Zhu, X. (2021). Hydrochemical characteristics and pollution source apportionment of the groundwater in the east foothill of the Taihang Mountains, Hebei Province. *Environment and Earth Science, 80*, 14. https://doi.org/10.1007/s12665-020-09341-4

Mukherjee, A., Saha, D., Harvey, C. F., Taylor, R. G., Ahmed, K. M., & Bhanja, S. N. (2015). Groundwater systems of the Indian sub-continent. *Journal of Hydrology: Regional Studies, 4*, 1–14. https://doi.org/10.1016/j.ejrh.2015.03.005

Naseem, S., Rafique, T., Bashir, E., Bhanger, M. I., Laghari, A., & Usmani, T. H. (2010). Lithological influences on the occurrence of high-fluoride groundwater in Nagar Parkar area, Thar Desert Pakistan. *Chemosphere, 78*(11), 1313–1321.

Ozsvath, D. L. (2009). Fluoride and environmental health: A review. *Reviews in Environmental Science and Bio/technology, 8*(1), 59–79.

Pi, K., Wang, Y., Xie, X., Su, C., Ma, T., Li, J., & Liu, Y. (2015). Hydrogeochemistry of co-occurring geogenic arsenic, fluoride, and iodine in groundwater at Datong Basin, northern China. *Journal of Hazardous Material, 300*, 652–661. https://doi.org/10.1016/j.jhazmat.2015.07.080

Rafique, T., Naseem, S., Ozsvath, D., Hussain, R., Bhanger, M. I., & Usmani, T. H. (2015). Geochemical controls of high fluoride groundwater in Umarkot sub-district, Thar Desert, Pakistan. *Science of the Total Environment, 530*, 271–278. https://doi.org/10.1016/j.scitotenv.2015.05.038

Rao, N. S., Dinakar, A., Sravanthi, M., & Kumari, B. K. (2021). Geochemical characteristics and quality of groundwater evaluation for drinking, irrigation, and industrial purposes from a part of hard rock aquifer of South India. *Environmental Science and Pollution Research*. https://doi.org/10.1007/s11356-021-12404-z

Rashid, A., Farooqi, A., Gao, X., Zahir, S., Noor, S., & Khattak, J. A. (2020). Geochemical modeling, source apportionment, health risk exposure, and control of higher fluoride in groundwater of sub-district Dargai. *Pakistan.*

Chemosphere, 243, 125409. https://doi.org/10.1016/j.chemosphere.2019.125409

Rashid, A., Guan, D.-X., Farooqi, A., Khan, S., Zahir, S., Jehan, S., Khattak, S. A., Khan, M. S., & Khan, R. (2018). Fluoride prevalence in groundwater around a fluorite mining area in the flood plain of the River Swat, Pakistan. *Science of the Total Environment, 635*, 203–215.

Rashid, A., Khan, S., Ayub, M., Sardar, T., Jehan, S., Zahir, S., Khan, M. S., Muhammad, J., Khan, R., & Ali, A. (2019a). Mapping human health risk from exposure to potential toxic metal contamination in groundwater of Lower Dir, Pakistan: Application of multivariate and geographical information system. *Chemosphere*. https://doi.org/10.1016/j.chemosphere.2019.03.066

Rashid, A., Khattak, S. A., Ali, L., Zaib, M., Jehan, S., Ayub, M., & Ullah, S. (2019b). Geochemical profile and source identification of surface and groundwater pollution of district Chitral, Northern Pakistan. *Microchemical Journal, 145*, 1058–1065.

Raza, M., Farooqi, A., Niazi, N. K., & Ahmad, A. (2016). Geochemical control on spatial variability of fluoride concentrations in groundwater from rural areas of Gujrat in Punjab Pakistan. *Environmental Earth Sciences*. https://doi.org/10.1007/s12665-016-6155-7

Reddy, A. G. S., Reddy, D. V., & Kumar, M. S. (2016). Hydrogeochemical processes of fluoride enrichment in Chimakurthy pluton, Prakasam District, Andhra Pradesh. *India. Environmental Earth Sciences, 75*(8), 5478. https://doi.org/10.1007/s12665-016-5478-8

Sagintayev, Z., Sultan, M., Khan, S. D., Khan, S. A., Mahmood, K., Yan, E., & Marsala, P. (2012). A remote sensing contribution to hydrologic modeling in arid and inaccessible watersheds, Pishin Lora basin, Pakistan. *Hydrological Processes, 26*(1), 85–99. https://doi.org/10.1002/hyp.8114

Saxena, V. K., & Ahmed, S. (2001). Dissolution of fluoride in groundwater: A water-rock interaction study. *Environmental Geology, 40*(9), 1084–1087.

Selvam, S. (2015). A preliminary investigation of lithogenic and anthropogenic influence over fluoride ion chemistry in the groundwater of the southern coastal city, Tamilnadu, India. *Environmental Monitoring and Assessment, 187*(3), 106. https://doi.org/10.1007/s10661-015-4326-8

Su, H., Wang, J., & Liu, J. (2019). Geochemical factors controlling the occurrence of high fluoride groundwater in the western region of the Ordos basin, northwestern China. *Environmental Pollution, 252*, 1154–1162. https://doi.org/10.1016/j.envpol.2019.06.046

Tahir, M. A., & Rasheed, H. (2013). Fluoride in the drinking water of Pakistan and the possible risk of crippling fluorosis. *Drinking-Water Engineering and Science, 6*(1), 17–23. https://doi.org/10.5194/dwes-6-17-2013

WAPDA. 2001. Water and power development authority. Individual basinal reports of Balochistan, Hydrogeology Project, Quetta, 1982–2000, Pakistan, Water, and Power Development Authority, Pakistan, Quetta

Wei, C., Guo, H., Zhang, D., Wu, Y., Han, S., An, Y., & Zhang, F. (2016). Occurrence and hydrogeochemical characteristics of high-fluoride groundwater in Xiji County, the southern part of Ningxia Province, China. *Environmental Geochemistry and Health, 38*(1), 275–290. https://doi.org/10.1007/s10653-015-9716-x

Wen, D., Zhang, F., Zhang, E., Wang, C., Han, S., & Zheng, Y. (2013). Arsenic, fluoride, and iodine in groundwater of China. *Journal of Geochemical Exploration, 135*, 1–21. https://doi.org/10.1016/j.gexplo.2013.10.012

WHO. (2011). Guidelines for drinking water quality. *World Health Organization, 216*, 303–304.

Zhang, Y., Ma, R., & Li, Z. (2014). Human health risk assessment of groundwater in Hetao Plain (Inner Mongolia Autonomous Region, China). *Environmental Monitoring and Assessment, 186*(8), 4669–4684. https://doi.org/10.1007/s10661-014-3729-2